Applied Mechanics and Materials
ISSN: 1662-7482, Vol. 885, pp 156-169
doi:10.4028/www.scientific.net/AMM.885.156

Submitted: 2018-06-21
Revised: 2018-07-25
Accepted: 2018-07-27
Online: 2018-11-20

Concept of a Resilient Process Chain to Control Uncertainty of a Hydraulic Actuator

Ingo Dietrich[1], Philipp Hedrich[1], Christian Bölling[2,a], Nicolas Brötz[1], Felix Geßner[2] and Peter F. Pelz[1,b]

[1]Chair of Fluid Systems, Otto-Berndt-Straße 2, 64287 Darmstadt, Germany,
[2]Institute of Production Management, Technology and Machine Tools, Otto-Berndt-Straße 2, 64287 Darmstadt, Germany

[a]boelling@ptw.tu-darmstadt.de, [b]peter.pelz@fst.tu-darmstadt.de

Keywords: resilience, process chain, digitalization, hydraulics, high precision machining

Abstract. Narrow tolerances are commonly used to control uncertainty in the production of technical components. However, they lead to financial expense and limit flexibility. In this paper, the concept of a resilient process chain is presented. This concept covers the product life cycle phases of production and usage. It is enabled by the digitalization in mechanical engineering and offers access to variable process windows instead of rigid tolerances. First steps of this concept are then applied to the TU Darmstadt's active air spring. The active air spring can be used to increase the driving comfort in a vehicle or, for instance, to minimize kinetosis during autonomous driving [1] [2]. The focus hereby is to identify possible production influences on the behaviour of the components usage. For this purpose, the actuator of the active air spring is specifically manufactured with typical uncertainty of high precision machining of the bore and characterized experimentally in a test rig. The results show an influence of the production on the efficiency of the actuator. The measurements are fundamental to establish a resilient process chain on the active air spring.

Introduction and Motivation

The roots of the industrial production of technical components go way back in time. In his book *The wealth of nations* Adam Smith describes how the division of labour increases the production of a pin manufactory [3]. In 1913 Henry Ford introduces the mass production. Fundamental to this success was the standardization and the control of processes. Hereby the increase of production goes hand in hand with the control of uncertainty. In 1987 Taguchi Gen'ichi reduced the sensitivity of process with his concept of Robust Design. All these approaches lead to the determination of tolerance windows for single parts, components and processes. However narrow process windows are expensive. Additionally, they reduce flexibility compared to the manufactury.

Since the past decade the upcoming digitalization offers increasing possibilities for the design of industrial production processes. With technologies like single part tracking and machine learning adaptive processes with variable process windows may be established. One approach for the design of adaptive processes is the concept of resilience. The goal is the consideration of uncertainty not only in the production itself, but also during the usage of the product. The history of industrial production processes leading towards adaptive processes is shown in figure 1.

In the third funding period, various projects within the Collaborative Research Center 805 "Control of Uncertainties in Load-Carrying Structures in Mechanical Engineering" address the effects of production-related uncertainty on the usage phase. The active air spring developed in the CRC is one of the objects under investigation. This paper first explains the general concept of a product life phase spanning resilient process chain. Subsequently, the functional prototype of the active air spring and current research on fine machining of bores using multi-blade reamers are explained. Then the concept of the resilient process chain is applied to the active part of the air spring, the hydraulic diaphragm actuator. In a first step, the knowledge of fine machining is used to apply typical production uncertainty

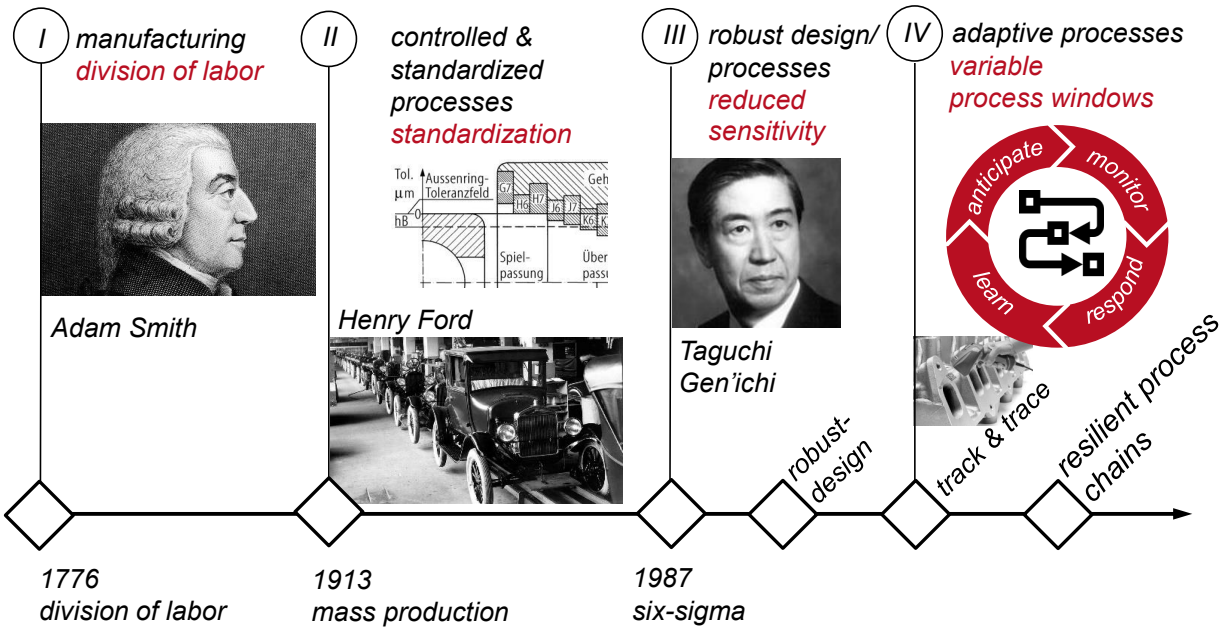

Fig. 1: The history of industrial production processes.

to the moving segments of the hydraulic diaphragm actuator. The effect of the introduced uncertainty on the characteristic behaviour of the air spring is then measured experimentally. The investigations are fundamental for modelling and implementing the resilient process chain to describe, evaluate and control uncertainty throughout product life phases.

Concept of a Product Life Phase Spanning Resilient Process Chain

In industrial environments, uncertainty in component production is countered by defining a tolerance band which, based on experience gained in development and application technology, is highly likely to ensure that the component produced will fulfill its function. The tolerance limits are usually defined against the direction of the value chain, starting with the finished part. The required tolerances of the preceding process steps are determined on the basis of empirical values. However, the accuracy requirements of earlier process steps are often subject to a subjective view. This procedure may lead to the definition of a narrow tolerance band, which leads to an increase in machining effort and thus to an increase in production costs. The focus is on the design of robust processes against previously considered sources of uncertainty. In industrial practice, there is often no quantification of the effect of production-related uncertainty on the usage phase which leads to nescience by ignorance.

Load-bearing structures have traditionally been developed for a specific design point. In the last decades numerous product recalls and failures led to the awareness that uncertainty is a part of every development, production and use of a technical product and cannot be neglected [4]. Common practice for dealing with this uncertainty is the robust design method. The next logical step is the resilient design of products that maintain a minimum function even in the event of failure of subcomponents or other effects that were not considered during design.

The concept of resilience cannot only be applied to control uncertainty during design, but also during operation and usage by integrating the four resilience functions monitoring, responding, learning and anticipating [5].

Resilience can be regarded as a paradigm shift: From designing systems and processes that are robust against a priori considerations, asking the question ”*what if...?*”, towards the design of systems and processes that perform ”*no matter what...*”.

Today the connection between the life phases production and usage is the product development. Customer feedback or guaranteed returns are analysed and the components life, described by operating and environmental parameters, is deduced. Ultimately the product or its production are changed to cope with the findings.

However, today an increasing number of technical products offers the possibility to collect data during the usage phase. Paired with the development of technologies like single part tracking and the increasing modelling of production processes and process chains, resilient product life phase spanning process chains become possible.

The concept of a product life phase spanning resilient process chain is shown in figure 2. Based on the production plan, a technical component is produced. The single production steps are described by models that use measured parameters during production. The same applies to the usage phase. (Soft-)sensors feed models which aggregate information during the usage. By a suitable selection of data that are logged during production as well as during usage they can be compared. By the feedback of the difference between actual data from the production and identificated data from the usage the models can be adapted and a learning function is established. Using time histories and correlating single part data to the respective usage data, the components behaviour can be anticipated already in the production itself. Based on this anticipation the usage plan of the component can be adapted.

The concept of a resilient process chain results in four requirements to the production and the component itself.

1. Production parameters must have an influence on the usage.
2. Data in the production and during usage must be collected.
3. Models that process the measured data from production and usage must exist.
4. Data that can be measured during production as well as during usage must be identificated.

Item 4 may require domain specific experience or empirical correlation between production and usage data that are not identical.

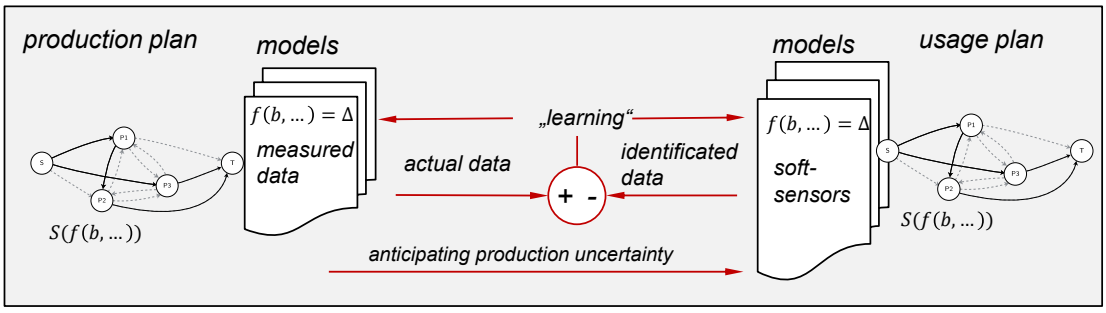

Fig. 2: Product life phase spanning resilient process chain.

The TU Darmstadt Active Air Spring

The TU Darmstadt active air spring is an active system that combines the advantages of air suspension, such as level control or the load-independent body eigenfrequency, with those of an active system that can actively reduce vibrations and has a flexible working area. For example, it can be used to minimize kinetosis during autonomous driving. The resulting compression force of the air spring is

$$F = (p - p_a)\, A_L, \tag{1}$$

with the pressure in the air spring p, the ambient pressure p_a and the load-carrying area A_L. There are two ways to actively execute the air spring — firstly an adjustment of the air spring pressure independent of the spring deflection or secondly an adjustment of the load-carrying area. A design evaluation showed that a controlled adjustment of the pressure, e.g. by increasing or decreasing the air spring volume, is too slow to realize required control frequencies of 5Hz. Adjusting the load-carrying area, on the other hand, is better suited for adjusting the axial force. Therefore, an active rolling piston was developed at the TU Darmstadt, whose radius r_P is hydraulically adjusted with four moving segments distributed over the lateral surface [6, 7, 1], Fig. 3.

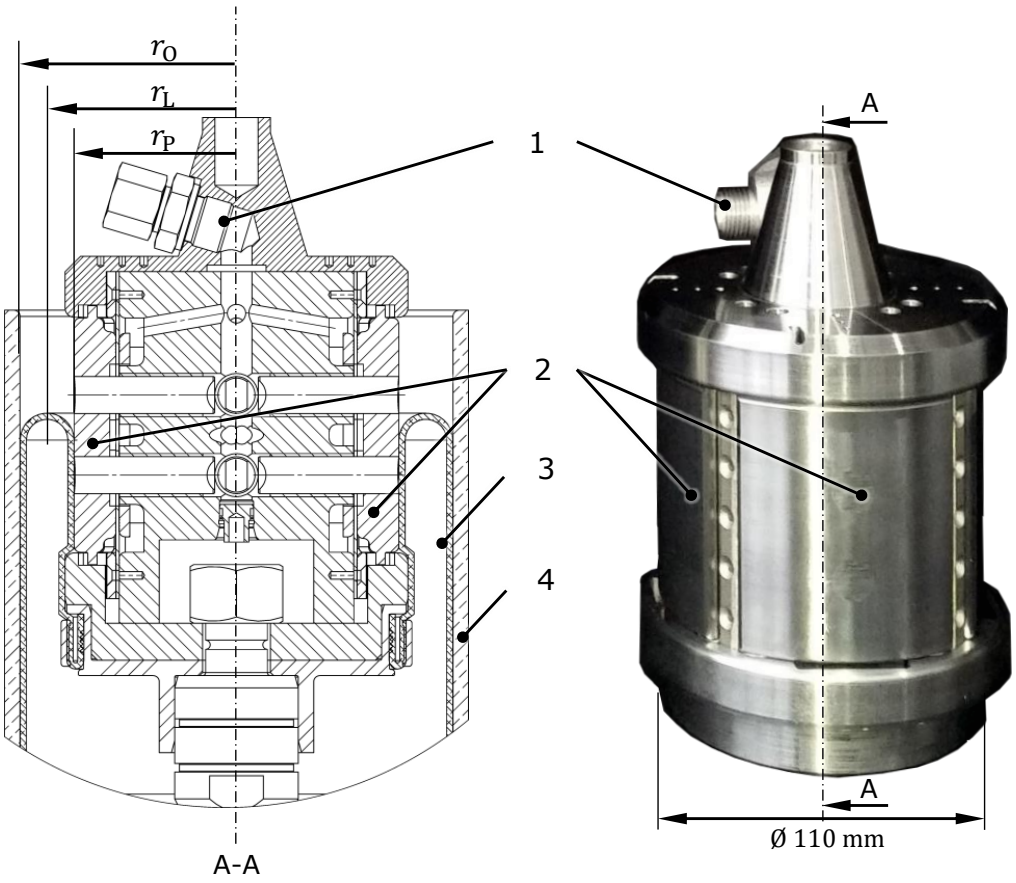

Fig. 3: The integrated hydraulic actuator can adjust the radius of the air spring rolling piston r_P, (1) is the hydraulic connection, (2) the adjustable segments, (3) the air spring bellows and (4) the outside guide of the air spring [8].

To maximize the axial force while simultaneously minimizing the power requirement, a double bellows air spring with a circular load-carrying area and two counter-rotating adjustable rolling pistons is used (Fig. 4). In order to increase the overall load-carrying area, the load-carrying area of the upper rolling piston is increased by extending the actuator and at the same time the lower load-carrying area is reduced by retracting the second actuator. The two actuators are controlled jointly by a double-acting cylinder. By moving the cylinder, one pressure chamber is enlarged and one is reduced - one actuator retracts and the other extends. The hydraulic system is dry because the chambers are closed and leakage-free. The concept enables the energy emitted during the automatic retraction of an actuator to be regenerated. This is fed directly to the extending actuator and only differential forces have to be set by the drive. The cylinder is currently driven hydraulically, but an electromechanical solution is also being worked on.

The actuating force of the prototype of the active air spring is $\pm 1000N$ at a static load of $2850N$. The load is adjusted by varying the air spring pressure and individualizing the control according to

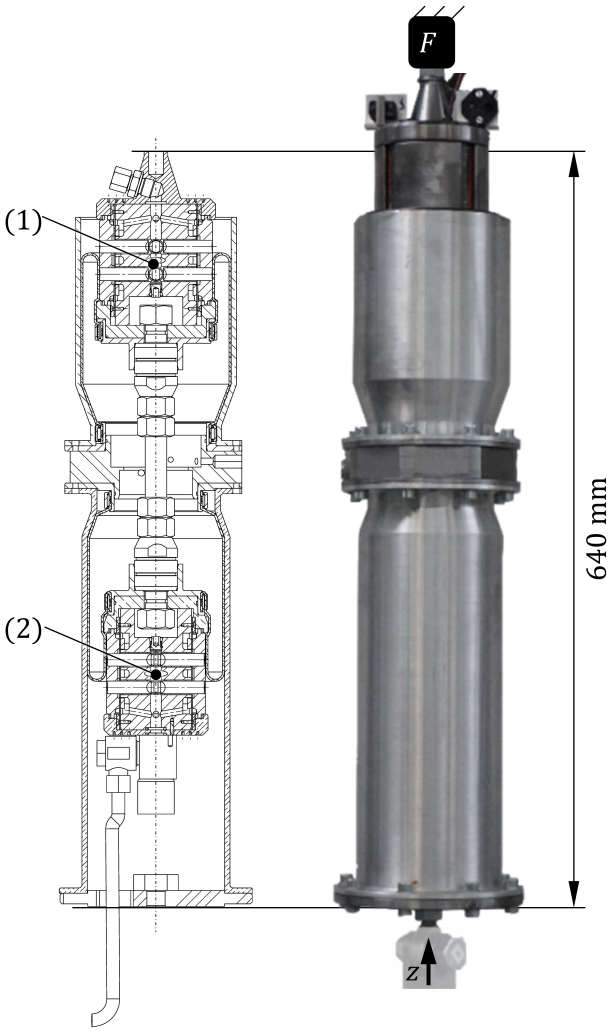

Fig. 4: The active air spring with two hydraulically adjustable rolling piston, labelled (1) and (2) [8].

the resilience principle “one size fits all”. Further important characteristics of the active air spring and the actuators can be taken from table 1.

The most important characteristics of the actuators were determined from generic theoretical preliminary investigations for active vertical dynamic vibration reduction on a quarter vehicle. First, the vibration reduction that can be achieved with an ideal active chassis was determined using mathematical optimization methods [8, 7, 9]. This ideal system represents a limit which, according to the motto “It doesn’t get any better!” cannot be bettered by any real system. From the requirement to improve the driving comfort with the active air spring, the required actuator axial force and positioning frequency could be determined from the preliminary investigations.

Then, various electrical, mechanical, pneumatic and hydraulic actuator concepts were examined in a concept study. It has been shown that a hydraulic actuator best meets the requirements due to its high power density. To remove torque, the segments are guided over two piston rods and run in sliding bearings. The pressure chamber is sealed at the segments with a diaphragm. This sealing concept was chosen because, in contrast to conventional ring seals, diaphragms have no leakage and are well suited for short-stroke applications [10]. The concept of the actuator is shown in the upper left in Fig.5 [11]. In addition to the round segments, flat segments are also available for investigations on a preliminary test bench.

Table 1: Parameters of the active air spring prototype. Index (1) refers to the upper rolling piston, index 2 to the lower one.

Parameter	Value
static pressure $p_{\mathrm{LF}}(z=0)$	$14\,\mathrm{bar(abs.)}$
outer radius r_{A1}	$70\,\mathrm{mm}$
rolling piston radius r_{K1}	$(52.5 \pm 3)\,\mathrm{mm}$
load-carrying area A_{T1}	$(11\,740 \pm 570)\,\mathrm{mm}^2$
outer radius r_{A2}	$63.5\,\mathrm{mm}$
rolling piston radius r_{K2}	$(47 \mp 2.5)\,\mathrm{mm}$
load-carrying area A_{T2}	$(9\,545 \mp 340)\,\mathrm{mm}^2$
total load-carrying area A_{T}	$(2\,195 \pm 910)\,\mathrm{mm}^2$
axial force $F(z=0)$	$(2\,850 \pm 1\,180)\,\mathrm{N}$
air spring volume V_0	$2.8\,\mathrm{l}$
maximal suspension travel z_{max}	$\pm 70\,\mathrm{mm}$

The sliding bearings in which the piston rods run are GLYCODUR F from Federal Mogul. These consist of a steel layer onto which a porous tin-bronze layer is sintered. The pores are filled with a PTFE layer. Finally, a running-in layer is applied, which is also made of PTFE. This layer transfers to the friction partner during operation. The bushes can be used both dry-running and lubricated. [12] Wear of the sliding layer increases the tolerance of the guidance during operation. For the lubricated use in the hydraulic actuator of the active air spring, no empirical values on wear are known.

The tolerances of the sliding bearings bring high demands on the bores in the actuator and the bores in the segments into which the piston rods are press-fitted. They determine the function of the actuator and will serve as an illustration of a resilient process chain within this paper.

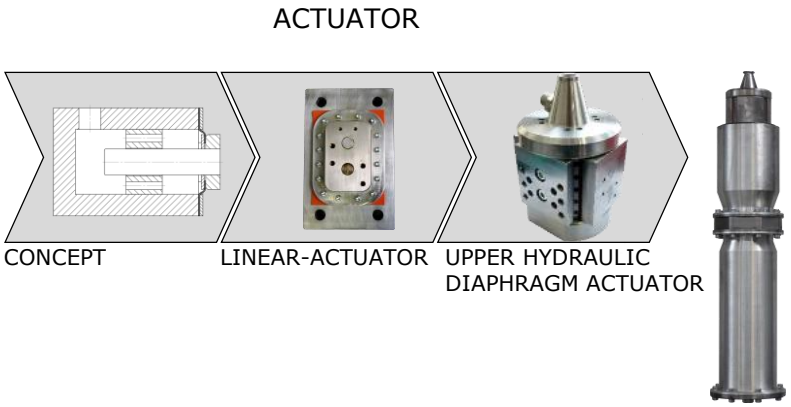

Fig. 5: Modules in the development of the active air spring.

Precision Machining of Bores with Multiblade Reamers

Typically, reaming within a process chain happens to the end of the value added to a product. Its purpose is to produce the shape and position of functional bores within the required tolerance range (DIN 8589 Part 2).

For productivity reasons nowadays often multiblade reamers are used where the functions ”cutting” and ”guiding” are combined in one geometric element [13]. The production of precision bores using multi-bladed reamers is the subject of various scientific studies. Uncertainty in the form of disturbances regularly influences the reaming process in industrial practice. Typical disturbances are

shown in figure figure 6. The influence of disturbances on the quality of the reamed bore has been investigated with regard to diameter, circular shape and cylindrical shape [14], [15] and with regard to the deflection of the tool [16], [17]. A deflection of the tool leads to an increased diameter of the casing cylinder of all bore centers of the reamed bore. The adjustment of the blade geometry by increasing the setting angle leads to a reduction in the deflection of the reamer during the transient entry phase into the work piece. An upstream pilot process significantly reduces the deflection, especially for long cantilevered tools with a length to diameter ratio of $L/D = 10$.

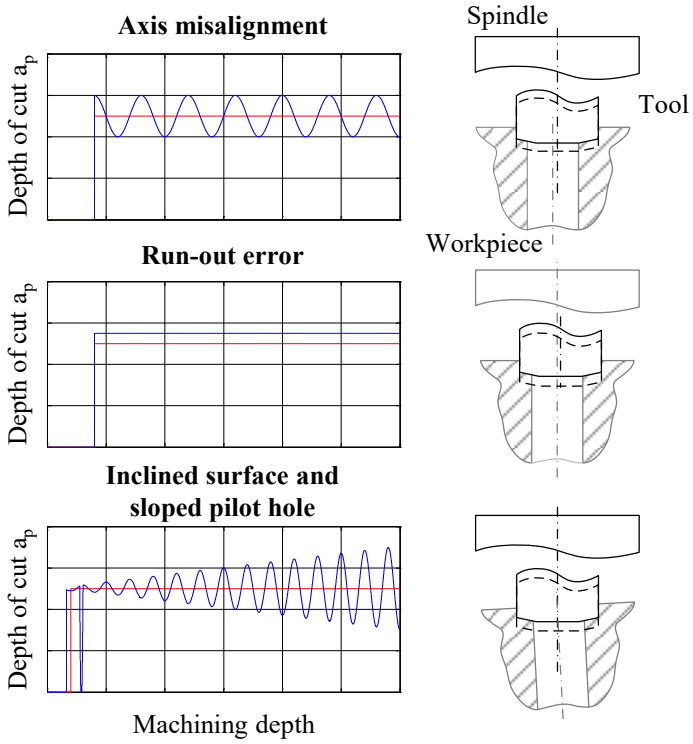

Fig. 6: Disturbances in the reaming process.

In the Collaborative Research Center 805, a simulation model for the analysis of multi-stage fine machining of bores has been developed and implemented. The simulation is based on an analytical model to calculate the undeformed chip cross-section [18], empirical cutting force models [19], [20] and a model to determine the tool behaviour. The tool model is based on the theory of the Laval rotor and the bar theory according to Bernoulli. The calculated chip cross-section at each single cutting edge results in the cutting forces F_c and passive forces F_p by means of an assignment rule, which, in turn, vectorially add up to a resulting radial force $F_r r$. Depending on the stiffness of the tool and the uncertainty it deflects the tool as it enters the work piece. This in turn leads to an increase of the casing cylinder of all bore centers [21].

The current object of research is the development of an online prediction model, which uses information from the respective individual processes via sensors for process control and final quality control. This means that an online quality prediction is available in the future.

Application of the Resilient Process Chain

Given the general concept, the method of the resilient process chain is applied to the hydraulic diaphragm actuator of the active air spring. The segments are produced at the Institute of Production Management, Technology and Machine Tools and assembled at the Chair of Fluid Systems. The usage

can be illustrated by component tests on a specially developed actuator test bench [6] or by using the actuator in the active air spring [7].

Based on the four requirements for the implementation of a resilient process chain, the influence of the production parameters on the usage is examined first. For this purpose, the knowledge gained in the CRC805 regarding precision machining of bores is used to introduce specific disturbances into the adjustable segments of the hydraulic actuator. The size and position of the bores are measured quantitatively using coordinate measuring technology. The hydraulic actuator is then assembled and characterized on the preliminary test bench. This characterization reflects the usage. According to figure 6 an axis misalignment of the bores in the segments is simulated. For this purpose, 3 different versions of the segments were produced. The distance of the holes in the segments (Figure 7) was varied by $\delta = [0; 60; 90]\ \mu m$. The results of the production were checked on a coordinate measuring machine. The axis misalignment was selected using the tolerances specified for the sliding bearings. The maximum offset corresponds to the maximum tolerance of the bore according to the data sheet [12]. This should ensure that the actuator can be assembled. The possible influences on the behaviour of the hydraulic actuator are changes in friction force and thus in the efficiency. For assembly with different segments, the synchronism of the segments movement could also be impaired.

In perspective, the whole resilient process chain from figure 2 can be represented for the hydraulic actuator as follows: The online prediction model, which is currently under development, for the precision machining of bores provides quality data of the produced segments and the actuator bores related to individual parts. The usage simulation in the preliminary test bench provides empirical data that can be correlated to these quality data. Based on this the production parameters or the models describing the production can be adjusted. On the other hand, the usage plan can be adjusted based on anticipation from the production data. For example, an individual maintenance interval could be defined for each actuator produced. During operation, the process pressure could be reduced to achieve a minimum service life. An individual nonlinear controller could also be conceivable, whose design or parameterization uses data from the online prediction model from the production.

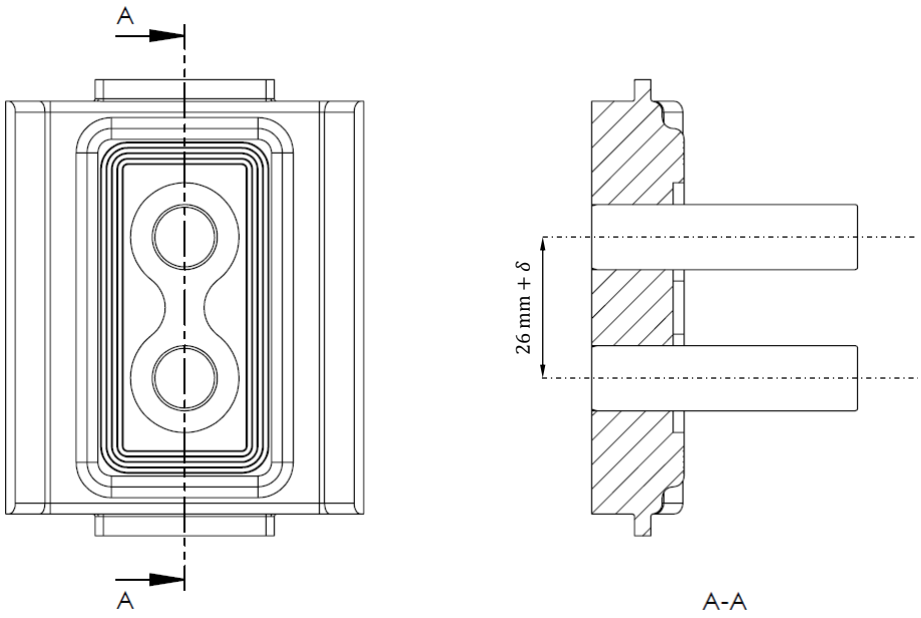

Fig. 7: The adjustable segments of the hydraulic diaphragm actuator that where induced with the disturbance δ simulating an axis misalignment according to Fig 6.

Table 2: Sensors used in the test rig.

Type	Name	Measuring Range
force	HBM 1C2/10kN	0...10 kN
displacement	Balluf BIP AD0-B014-01-EP02	-7...7 mm
pressure in the actuator	Keller PA-4LC/80843.9	0...50 bar
pressure upstream of the valve	Keller PA-23/8465-100	0...100 bar
pressure downstream of the valve	Keller PA-23/8465-100	0...100 bar
temperature of the oil	Hydac ETS 4146-B-006-000	-25...100 °C

Experiments

In order to minimize influences from the assembly on the final result, an instruction was created and the actuator was assembled accordingly by the same persons. When changing the segments, new bearings were pressed in to counteract uncertainty due to the running-in behaviour. The configuration $\delta = 90\mu m$ was mountable, but only with great force. Therefore it was not evaluated. Theoretically the tolerances of the bearings should allow a smooth mouting, however the body of the actuator cannot be expected to be without any tolerances due to manufacturing.

The previous preliminary test rig [6] was further developed to characterize the hydraulic actuator (see Figure 8). The load unit used to consist of plunger cylinders. In order to minimize possible influences from friction forces in the cylinders, two connected air springs are now used. The load is adjusted via the internal air spring pressure. The actuator is attached to the test rig via two closed sides, thus leaving two moving segments. The proportional valve *4WRPE 6 E 32SJ-576 10th2X/G24K0/A1MA* from Bosch Rexroth is used to control the displacement of the hydraulic actuator with a PI controller. The valve control and data acquisition is realized via a *dSpace 1202* system. For all experiments, Shell Tellus S2M 46 HLP oil with a measured density of $\varrho = 0.879$ kg/l at 40 °C was used. An overview of the sensors is given in table 2.

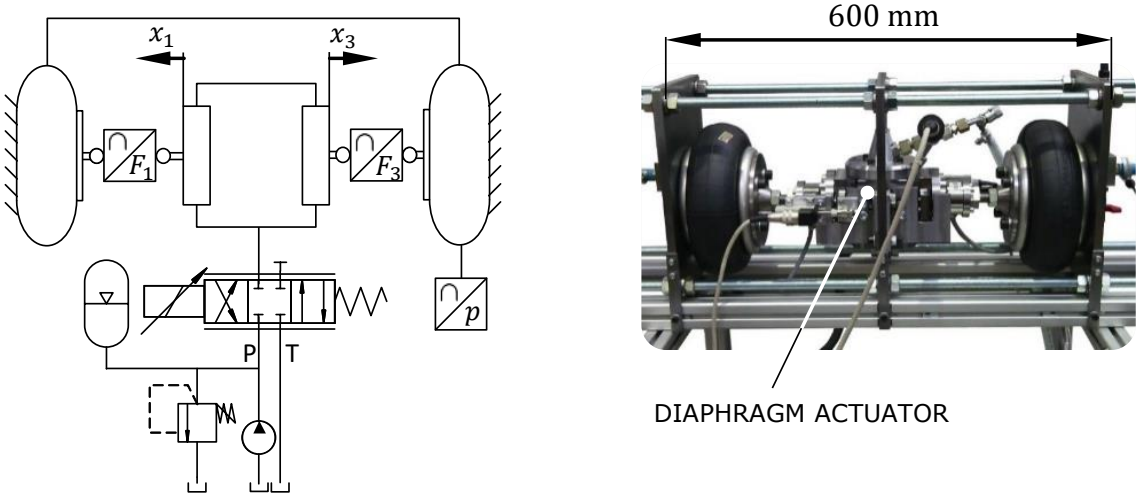

Fig. 8: Test rig and hydraulic schematic diagram [22].

Different test parameters were used to characterize the actuator with the different configurations of segments and body. All test parameters are listed in table 3.

Parameters characterizing the hydraulic actuator can be calculated from the tests carried out. Friction force and efficiency are of particular interest for the operation in the active air spring. Both parameters must be calculated from the available measured variables. The equation of linear momentum at the piston with the measured force F_{m}, hydraulic force F_{hyd}, segment position x and the weight of the moving segment m_{A} writes to

Table 3: Test parameters.

Parameter	Values
static load centric	$F_0 = 4\,\mathrm{kN}$
	$T_0 = 0\,\mathrm{Nm}$
static load excentric	$F_0 = 4\,\mathrm{kN}$
	$T_0 = 66\,\mathrm{Nm}$
amplitude	$\hat{x} = (0.1...2)\,\mathrm{mm}$
offset	$x_0 = (-2...2)\,\mathrm{mm}$
frequency	$f = (0.1...10)\,\mathrm{Hz}$

$$F_{\mathrm{m}} = F_{\mathrm{hyd}} - F_{\mathrm{F}}\mathrm{sgn}(\dot{x}) - m_{\mathrm{A}}\ddot{x}. \tag{2}$$

The hydraulic force F_{hyd} can be calculated from the load-carrying area A_{L} and the differential pressure between the actuator and the environment Δp_{hyd} through

$$F_{\mathrm{hyd}} = A_{\mathrm{L}}\Delta p_{\mathrm{hyd}}. \tag{3}$$

As the authors have shown in [6] the load-carrying area depends on the segment position x through membrane buckling. To determine A_{L} a harmonic measurement is evaluated at a frequency of $10Hz$ and $0.1mm$ amplitude. The harmonic signal and averaging the measured force F_{m} simplifies equation 2 and the load-bearing area is defined as

$$A_{\mathrm{L}} := \frac{\bar{F}_{\mathrm{m}}}{\Delta p_{\mathrm{hyd}}}. \tag{4}$$

To avoid dynamic influences, the friction force F_{F} is determined with a quasistatic measurement at an excitation frequency of $f = 0.1Hz$. The friction force is defined as

$$F_{\mathrm{F}} := \frac{W_{\mathrm{dis}}}{4\hat{x}} = \frac{\oint F_{\mathrm{hyd}}\,\mathrm{dx}}{4\hat{x}} \tag{5}$$

with the dissipated Energy W_{dis} and the amplitude $\hat{x}$.

Dynamic influences are taken into account to determine the efficiency η. With the input energy W_{in} and the dissipated energy W_{dis} it is defined as

$$\eta := \frac{W_{\mathrm{in}} - W_{\mathrm{dis}}}{W_{\mathrm{in}}}. \tag{6}$$

Figure 9 shows the determination of the input Energy W_{in} and the dissipated energy W_{dis}.

Figure 10 shows the amplitude and frequency dependent efficiency with centric load for the axis misalignment of $\delta = 0\mu m$ and $\delta = 60\mu m$. The efficiency for the segments with axis misalignment is below the assembly without axis misalignment at all operating points. The average efficiency without axis misalignment is $\eta_{c,\delta=0\mu m} = 0.97$ and for the segments with misalignment $\eta_{c,\delta=60\mu m} = 0.95$. This result seems plausible, since the linear load on the sliding bearings is increased by the misalignment.

For the measurements with excentric load, the efficiency is shown in figure 11. As already shown in previous tests, the efficiency with excentric load is below the one for centric load [6]. This also applies to the configuration with axis misalignment. In contrast to the centric load, the efficiency without misalignment $\eta_{d,\delta=0\mu m}$ is below the efficiency with misalignment $\eta_{d,\delta=60\mu m}$ for almost all operating points. This is also reflected in the average efficiencies $\eta_{d,\delta=0\mu m} = 0.92$ and $\eta_{d,\delta=60\mu m} = 0.93$.

An examination of the force hysteresis as an indicator for the friction force in figure 12 confirms the results of the efficiency evaluation. For better comparison a substitute force is plotted.

$$F_{\mathrm{Shyd}} := F_{\mathrm{hyd}} - \bar{F}_{\mathrm{hyd}} \tag{7}$$

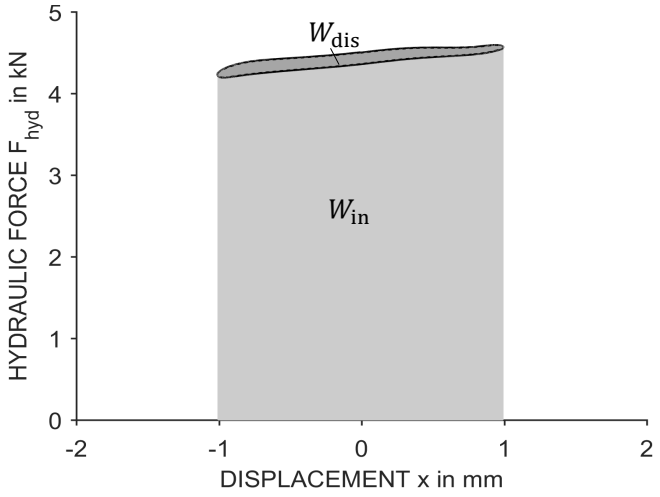

Fig. 9: Determination of the input Energy W_{in} and the dissipated energy W_{dis}.

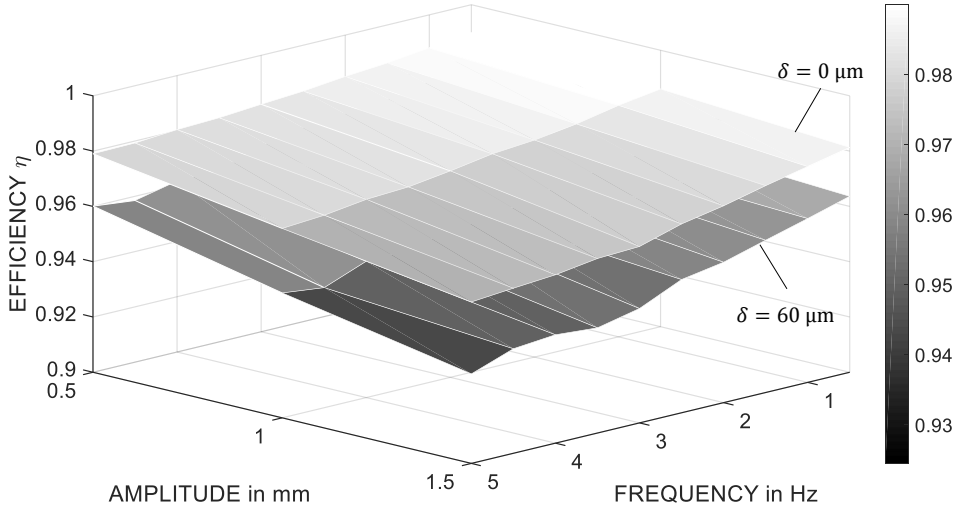

Fig. 10: Comparison of the efficiencies for the measurements with centric load at harmonic excitation $x = \hat{x}\sin(2\pi ft)$.

The friction force with centric load is lower in both configurations than the friction force with excentric load. The friction force for the configuration $\delta = 60\mu m$ is, however, lower for the installation with an excentric load. Table 4 shows the values for the friction force F_{F}.

In principle, the investigations show that there is an influence of the axis misalignment on the friction forces and thus on the efficiency. However, the effects cannot be clearly described. The improvement in efficiency for the installation with excentric load cannot be explained at first. One factor might be the uncertainty during assembly, another might be uncertainty in the sliding bearings which would affect the friction behaviour. Before the experimental investigation of further manufacturing defects, these other influencing factors must be ruled out.

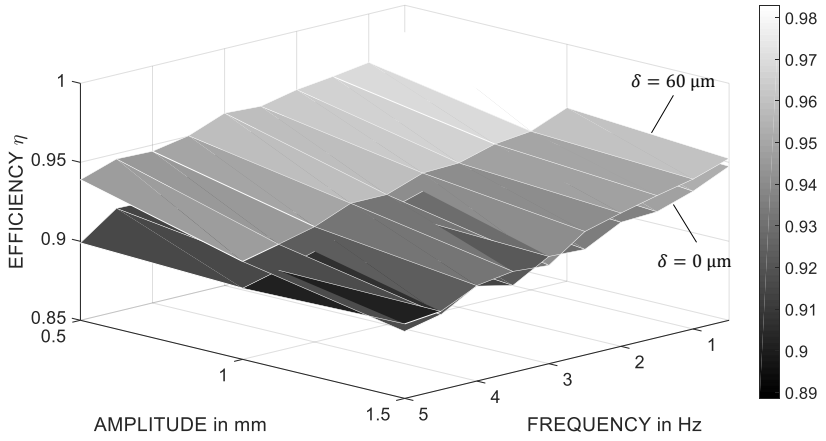

Fig. 11: Comparison of the efficiencies for the measurements with excentric load at harmonic excitation $x = \hat{x}\sin(2\pi ft)$.

Table 4: Measured Friction Forces.

Load	$\delta = 0\,\mu$m	$\delta = 60\,\mu$m
centric	20.3 Nm	26.9 Nm
excentric	56.7 Nm	42.3 Nm

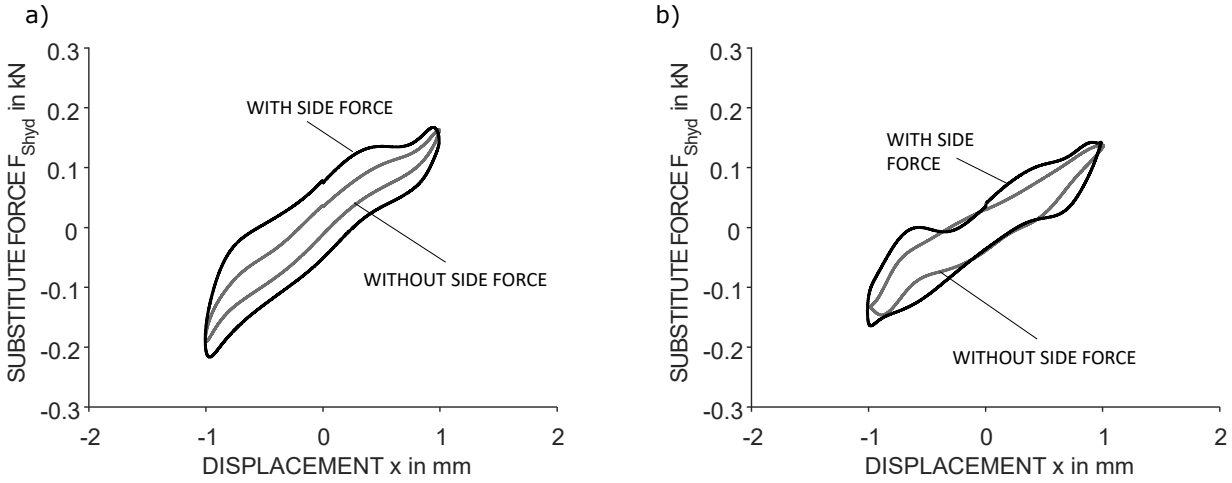

Fig. 12: Comparison of the friction force over the displacement for a) the configuration $\delta = 0\mu m$ and b) the configuration $\delta = 60\mu m$.

Summary and Outlook

In this paper the concept of a product life phase spanning resilient process chain is presented. It is enabled by the digitalization in mechanical engineering and represents a possibility to operate processes with variable process windows instead of fixed tolerances.

Within the scope of the cooperation in the Collaborative Research Center 805, first steps were taken to apply the described concept to a component of the TU Darmstadt active air spring, the hydraulic diaphragm actuator. Findings from the Collaborative Research Center 805 on the precision machining of bores were used to introduce specific disturbances into the hydraulic membrane actuator. The influences on the efficiency were investigated in experimental tests.

The results show that there is an influence of the precision machining of the bore on the efficiency of the actuator, but it cannot be clearly explained. It is likely that there are influences of the bearings or the assembly process which must be excluded before further investigations are carried out. Subsequently, the influence of further manufacturing defects can be investigated. With the help of a larger database, an empirical correlation between production and usage can then be established.

In the further cooperation it is planned to implement a link of the production processes with the usage scenarios in an online model. For the production process this development aims at the implementation of a data-based process control and quality assessment. The results from linking the production and the usage are then to be used in order to make adjustments within the production process chain automatically and thus to control uncertainty. Therefore machine learning methods are to be combined with the developed prediction models.

Acknowledgment

The authors would like to thank the German Research Foundation, DFG, for funding this research within the Collaborative Research Center SFB 805 ”Control of Uncertainties in Load-Carrying Structures in Mechanical Engineering”.

References

[1] Dj.M. Maric, P.F. Meier and S.K. Estreicher: Mater. Sci. Forum Vol. 83-87 (1992), p. 119

[2] P. Hedrich, E. Lenz, and P. F. Pelz. “Besser geht’s nicht - Pareto-optimale aktive Vertikaldynamiktechnologie zur Minimierung von Kinetose beim autonomen Fahren (akzeptiert)”. In: ATZ - Automobiltechnische Zeitschrift 120.7 (2018).

[3] P. Hedrich, E. Lenz, and P. F. Pelz. “It doesn’t get any better - Pareto-optimal Active Vertical Dynamics Technology for Mitigating Kinetosis during Autonomous Driving”. In: ATZ Woldwide 120.7 (2018).

[4] A. Smith. An Inquiry into the Nature and Causes of the Wealth of Nations. Scotland, Great Britain, 1776.

[5] M. S. Phadke. Quality engineering using robust design. 1995.

[6] E. Hollnagel. “Prologue: The Scope of Resilience Engineering”. In: Resilience Engineering in Practice: A Guidebook. Ed. by E. Hollnagel, J. Pariès, D. D. Woods, and J. Wreathall. Ashgate Studies in Resilience Engineering. Boca Raton, Florida: CRC Press, 2011, pp. xxix–xxxix.

[7] P. Hedrich, M. Johe, and P. F. Pelz. “Design and Realization of an Adjustable Fluid Powered Piston for an Active Air Spring”. In: 10th International Fluid Power Conference. Vol. 1. 2016, pp. 571–582.

[8] P. Hedrich, N. Brötz, E. Lenz, and P. F. Pelz. “Active Pneumatic Suspension for Future Autonomous Vehicles: Design, Prove of Concept and Hardware-in-the-Loop Simulations”. In: 11th International Fluid Power Conference. Vol. 3. 2018, pp. 352 –365.

[9] P. Hedrich, E. Lenz, and P. F. Pelz. “Modellbildung, Regelung und experimentelle Untersuchung einer aktiven Luftfederung in einer Hardware-in-the-Loop-Simulationsumgebung”. In: VDI-Fachtagung Schwingungen. VDI-Berichte. 2017, pp. 447–460.

[10] E. Lenz, P. Hedrich, and P. F. Pelz. “Aktive Luftfederung – Modellierung, Regelung und Hardwarein- the-Loop-Experimente (akzeptiert)”. In: Forschung in Ingenieurwesen (2018).

[11] H. K. Müller. “Hermetische Dichtungen”. In: Abdichtung bewegter Maschinenteile. Ed. by H. K. Müller. Waiblingen: Springer Berlin Heidelberg, 1990, pp. 243–251.

[12] P. Hedrich, M. Johe, and P. F. Pelz. “Aktor mit einem linear verlagerbaren Stellglied”. Patent DE 102015120011 A1. May 18, 2017.

[13] F. Mogul. GLYCODUR Dry bearings. data sheet. Federal Mogul, 2013.

A. Basteck. Einsatzgebiete des Reibens bei der Hochgeschwindigkeitsbearbeitung und Trockenzerspanung. Schmalkalden, 1994.

[14] O. Bhattacharyya, S. G. Kapoor, and R. E. DeVor. “Mechanistic model for the reaming process with emphasis on process faults”. In: International Journal of Machine Tools and Manufacture 46.7-8 (2006), pp. 836–846.

[15] F. Koppka. A contribution to the maximization of productivity and workpiece quality of the reaming process by analyzing its static and dynamic behavior. An analysis with focus on automotive powertrain production. Aachen, 2009.

[16] T. Hauer. Modellierung der Werkzeugabdrängung beim Reiben - Ableitung von Empfehlungen für die Gestaltung von Mehrschneidenreibahlen. Aachen, 2012.

[17] C. Bölling, S. Güth, and E. Abele. “Control of uncertainty in high precision cutting processes: Reaming of valve guides in a cylinder head of a combustion engine”. In: Applied Mechanics and Materials 807 (2015), pp. 153–161.

[18] E. Abele and C. Bölling. “Modellierung der geometrischen Eingriffsbedingungen bei der Ventilsitzbearbeitung am Zylinderkopf”. In: Werkstatttechnik online: wt 104.11/12 (2014), pp. 735–740.

[19] E. Abele, T. Hauer, and M. Haydn. “Modellierung der Prozesskräfte beim Reiben mit Mehrschneidenreibahlen - Implementierung eines Kraftmodells für die Simulation der Reibbearbeitung”. In: Werkstattstechnik online: wt 101 (2011), pp. 407–412.

[20] C. Bölling, M. Kuhne, and E. Abele. “Modeling of Process Forces with Consideration of Tool Wear for Machining of Sintered Steel Alloy for Application to Valve Seat in a Combustion Engine”. In: Production Engineering: WGP 11.4-5 (), pp. 477–485.

[21] C. Bölling, F. Hoppe, F. Geßner, M. Knoll, E. Abele, and P. Groche. “Fortpflanzung von Unsicherheit in Prozessketten”. In: Werkstatttechnik online: wt 108.1/2 (2018), pp. 82–88.

[22] P. Hedrich. “Konzeptvalidierung einer aktiven Luftfederung im Kontext autonomer Fahrzeuge”. Dissertation. Technische Universität Darmstadt, 2018.